

## RED SUPERGIANTS IN M 31: EXTINCTION, METALLICITIES AND GAS-TO-DUST RATIO

PETKO NEDIALKOV and TODOR VELTCHEV

*Department of Astronomy, University of  
Sofia, James Bourchier 5, Sofia 1164, BULGARIA*

*E-mail japet@phys.uni-sofia.bg*

*E-mail eirene@phys.uni-sofia.bg*

**Abstract.** We derived individual extinction values for selected red supergiant (RSGs) candidates in M31 with broadband photometry. Taking into account their position on the colour-magnitude diagram and using a probability method, the metallicity of each star was estimated. In the range 2-15 kpc the ratio  $[O/H]$  is nearly constant. The derived individual extinctions and pencil beams values from three different gas maps (Westerbork HI, VLA HI and IRAM CO(1 $\rightarrow$ 0)-line survey) were used to obtain gas-to-dust ratio in M31. For the 9 most luminous stars both the ratios  $N(HI)/2 E_{B-V}$  and  $N(HI + H_2)/2 E_{B-V}$  are not very different from those in the Milky Way. Significant fractions outside the expected range of Galactic atomic gas-to-dust ratio are obtained for  $\sim 1/3$  of the sample using Westerbork and for  $\sim 1/2$  of the sample - using VLA maps. The ratios are overestimated for objects located high above the midplane of M31 and underestimated - due to resolution effects, - for several RSGs coinciding with small HI clouds.

### 1. INTRODUCTION

The available broadband photometry for RSGs in nearby galaxies offers a good opportunity for the derivation of their extinction through the Q-method. On a colour-colour diagram containing  $(V - I)$  colour, these objects are distinctly separated from the foreground dwarfs and the position of the zero-absorption line allows unambiguous determination of their true colour. The aim of our work is to obtain individual extinctions and metallicities for RSGs in M31 that can be used to study the gas-to-dust ratio.

### 2. THE SAMPLES AND THE DEREDDENING PROCEDURE

The main source of objects for the present study is the large catalog with BVRI photometry of Magnier et al. (1992). The diagrams  $(B - V)$  vs.  $(V - I)$  (Fig. 1) and  $(V - R)$  vs.  $(V - I)$  (Fig. 2) clearly show the red end of the foreground dwarfs sequence whose scatter increases with the V magnitude. The zero-absorption line for supergiants was composed as a strip encompassing the Geneva evolutionary tracks (Lejeune & Schaerer 2001) for masses in the typical range of 9-25  $M_{\odot}$ . In both Figures, the thin lines designate the borders of the strip and the thick one - its center.

We adopted the Galactic value of the total-to-selective-extinction ratio  $R_V = 3.1$  leading to a slope of the reddening vector as plotted in the lower left corners. Then the true colour of each star is calculated through the Q-method for 9 different sets of colour values corresponding to the central point, the corners and the size-centers of its photometric error box, and for the two borders and central line of the zero-absorption line strip: 27 values in total. The error of the true colour is obtained as arithmetic mean of its minimum and maximum value. However, the position and photometric errors of some objects below the strip do not allow derivation of plausible values in all 27 cases. We chose RSG candidates that allow at least 9 dereddenings with the adopted slope: 64 on diagram  $(B-V)$  vs.  $(V-I)$  (Fig. 1) and 35 on diagram  $(V-R)$  vs.  $(V-I)$  (Fig. 2). To the common objects was ascribed a colour excess that is the average value obtained from both diagrams. Finally we have 69 RSG candidates of the catalog of Magnier et al. (1992) with reliably determined true colours and extinction. Five of them turn out to be very luminous and were excluded from the study of the metallicity gradient and gas-to-dust ratio in the galaxy (see next section).

The second source for RSG candidates is a list of red stars in M31 of Massey (1998). His BVR photometry is of higher precision and we supplemented it - after a cross-identification, - only with an I magnitude from the catalog of Magnier et al. (1992). Thus further 37 objects were selected (not included in the first sample) appropriate for dereddening through our procedure both on the diagram  $(B-V)$  vs.  $(V-I)$  and/or  $(V-R)$  vs.  $(V-I)$ .

### 3. EXTINCTION AND METALLICITY OF THE RSG-CANDIDATES IN M31

The derived individual extinctions  $A_V$  for the RSGs are not high and vary from 0.2 to 2.2. Their lower limit is close to the foreground extinction toward M31 of  $E_{B-V} = 0.062$  (Schlegel et al. 1998). The assumed distance modulus is 24.47 (Stanek & Garnavich 1998). As shown in Fig. 3, the absolute magnitudes of most RSG candidates fall into the range  $-5 > M_V > -7$  (initial masses 12-21  $M_\odot$ ) which supports the claim that there is a lack of luminous RSGs in the Andromeda galaxy (Berkhuijsen & Humphreys 1989, Massey 1998). There are five exceptions with true colours  $(V-I)_0 \sim 2.0$ , located in an area where the evolutionary tracks for more massive stars reach their turning point to the blue. These very luminous objects from the catalog of Magnier et al. (1992) are most likely affected by blending which is pointed out as a problem of this photometry. The evolutionary tracks of the RSGs on the colour-magnitude diagram and their lifetimes turn out to depend essentially on the star's metallicity  $Z$  (see e.g. Salasnich, Bressan & Chiosi 1999). Thus the probabilities to "meet" in a fixed area a RSG with given  $Z$  vary significantly which enables us to estimate the individual metallicity via a simple 'bullets-method' (Fig. 4). The location of a star on the diagram  $M_V$  vs.  $(V-I)$  is determined by its error box which is crossed through by tracks for different sets of initial masses  $M$  and  $Z$ . We calculated approximate tracks in the mentioned range of 9-25  $M_\odot$  with step  $\Delta M = 1$  as functions of  $M$  and  $Z$  using the analytic formulae of Hurley, Pols & Tout (2000). The initial stellar mass is out of scope of this work and we consider  $Z$  as the sole parameter. If each track is divided by points of one and the same, fixed timestep, the number of points  $N_{Z_i}$  for metallicity  $Z_i$  ('bullets of type  $Z_i$ ') in the

error box would be a measure for the probability that the stellar metallicity is  $Z_i$ :

$$p_i = N_{Z_i}/N$$

where  $N$  is the total number of points in the error box. Then the estimates of the individual metallicity and its error are given by:

$$Z = \sum_i p_i Z_i$$

$$\sigma_Z = \sqrt{\frac{\sum_i N_{Z_i} Z_i^2 - Z^2}{N}}$$

The total metallicity  $Z$  was transformed to  $[O/H]$  assuming relative element abundances as derived by Anders & Grevesse (1989) for the solar photosphere. The obtained values are plotted vs. the galactocentric distance of the RSGs in Fig. 5. There is no evidence for a steep metallicity gradient in M31 in the range  $10' - 70'$  (2-15 kpc). For comparison are drawn the gradients of Smartt et al.(2001) ( $-0.018 \text{ dex kpc}^{-1}$ ) and Galarza, Walterbos & Braun (1999) ( $-0.06 \text{ dex kpc}^{-1}$ ) used two different abundance calibrations for the  $HII$  regions. Our result becomes clearer if we require stronger criteria concerning the dereddening procedure: at least 18 plausible dereddenings of 27 possible and at least 4 plausible dereddenings to each border and to the central line of the zero-absorption strip (see Fig. 1 and 2). We then obtain a subsample with highly reduced scatter of abundance estimates vs. galactocentric distance (filled symbols, Fig. 5). Up to angular distances of  $\sim 30'$ , there may be a slight positive gradient  $[O/H]$ . In the region between  $30'$  and  $65'$  (7-15 kpc) the stellar metallicity varies in a wide range above the predicted values with the same scatter like in the abundance studies mentioned above. This may indicate that objects with different metallicities are present even at a fixed galactocentric distance. One possible explanation is the enrichment of the protostellar matter due to ongoing active star formation and consequent supernova explosions. Recently this ring of active star formation has been a subject of intensive research (e.g. Pagani et al. 1999).

#### 4. GAS-TO-DUST RATIO IN M31

The new CO(1 $\rightarrow$ 0) map (Guélin et al. 2000) with a spatial resolution of  $23''$  at  $\lambda$  2.6 mm combined with the available  $HI$  maps of M31 yields excellent opportunities for detailed study of the total gas-to-dust ratio. Here we mean by 'dust' the derived individual extinction values for the RSGs. Because of the poor statistics (106 extinction estimates) it is not possible to construct an extinction map. For the atomic hydrogen we took pencil beam column densities at  $\lambda$  21 cm from 2 different maps: Westerbork with an angular resolution of  $24 \times 36''$  (Brinks & Shane, 1984) and VLA with a resolution of  $10''$  (Walterbos & Braun, 1992). As the VLA map does not cover a large part of the SW half of M31 and further only the extinctions of 55 objects falling in both maps are considered. We converted CO-intensity to molecular hydrogen column density  $N(H_2)$  using a constant  $X_{CO}$  conversion factor (Strong & Mattox 1996) since the metallicity is nearly constant with radius. The total column density  $N(HI + 2H_2)$  is obtained as the sum of both components, multiplied by a factor 1/2 assuming that the stars on the average are located at the midplane of the galaxy. The relationships 'atomic gas-dust' and 'total gas-dust' are illustrated in Fig. 6 and Fig.

7, respectively. A constant gas-to-dust ratio in M31 would yield a good correlation like in the Milky Way (cf. Fig. 2 in Bohlin et al. 1978) which is not the case here. One of the explanations could be a gas-to-dust ratio depending on the galactocentric distance. But the observed large spread is most probably due to another reason: the varying fraction of the gas density (not exactly 1/2) associated with the dust – stars located in the front part or in the back of the disk yield deviations from the corresponding line. To diminish the latter effect we divide our sample in 3 different groups on the diagram  $HI$  vs.  $E_{B-V}$  (Fig. 6): objects within (filled triangles), above (open squares) and below (open circles) the expected range of the Galactic ratio. The most luminous objects (large open squares) with a single exception due to resolution problems (see below) turn out to be members of the first group. The single criterion  $M_V < -6$ , immediately improves the correlations for limited samples in magnitude used here since such stars can be seen even under larger column densities of the gas. On the other hand, the presence of objects with overestimated gas-to-dust ratio (open squares; the typical deviating case) is explained with their high location above the galactic midplane. The objects within the expected range of Galactic atomic gas-to-dust ratio are most appropriate for a study of total gas-to-dust ratio (Fig. 7). This group is obviously larger in number using the Westerbork data (left hand panel, 60% of the sample). Following Bohlin et al. (1978), one should expect that adding of the molecular gas fraction will tighten the ‘total gas-dust’ correlation. This effect is not seen in Fig. 7, however. One notes that the VLA data (right hand panel) have less scatter around the line corresponding to the Galactic total gas-to-dust ratio. That leads us to a third reason for decreasing the expected correlation: the angular resolution of the  $HI$  maps. Direct comparison in Fig. 6 between Westerbork (left hand panel) and VLA (right hand panel) column densities shows a scale difference of  $\sim 2$ . A natural explanation may be that the ISM in M31 consists predominantly of small clouds not well resolved on the Westerbork map. Indeed, the RGSs lying below the expected strip (open circles in the left hand panels) are located in such small clouds with underestimated column density on  $24 \times 36''$  resolution map.

The calculated estimates of the gas-to-dust ratios based on the data for 9 most luminous RGSs (8 on the right hand panels) are summarized in Table 1. It is intriguing that the values of Lequeux (2000) for the outermost part of M31 are significantly higher while the canonical Galactic values (Bohlin et al. 1978) are confirmed by our results. For further details, comments and discussion see our forthcoming paper.

*Acknowledgments.* We thank Elly M. Berkhuijsen for a fruitful discussion and the valuable comments on the manuscript. This research was partially supported by contract Nr. F-825/1998 with the National Science Foundation, Ministry of Education and Sciences, Bulgaria.

Table 1: Gas-to-Dust Ratios in M31 and in the Milky Way

	$\langle N(\text{HI})/2E_{\text{B-V}} \rangle$ [ $10^{21}$ atoms $\text{cm}^{-2}$ mag $^{-1}$ ]	$\langle N(\text{HI} + 2\text{H}_2)/2E_{\text{B-V}} \rangle$ [ $10^{21}$ atoms $\text{cm}^{-2}$ mag $^{-1}$ ]
Westerbork	$1.4 \pm 0.4$	$3.4 \pm 1.1$
VLA	$5.7 \pm 1.9$	$5.9 \pm 2.0$
M31 (Lequeux 2000)	$11.0 \div 14.5$	—
Milky Way (Bohlin et al. 1978)	$4.8 (1.5 \div 14.5)$	$5.8 (3.3 \div 10)$

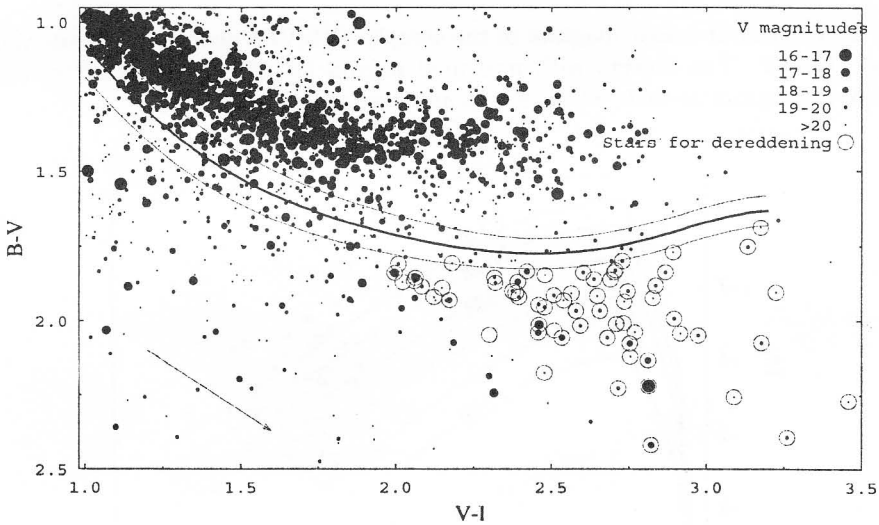


Fig. 1: The colour-colour diagram of the sample with BVI photometry from Magnier et al. (1992). The point sizes correspond to different V magnitude intervals. In the lower left is shown the direction of the reddening vector ( $R_V = 3.1$ ). The strip delineated with solid lines gives the location of the zero-absorption line (see text). The stars appropriate for our dereddening procedure are plotted with open circles.

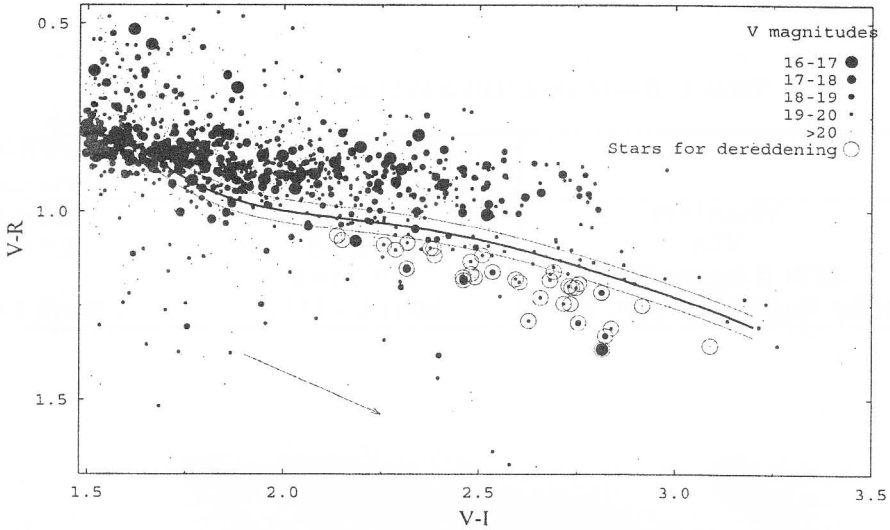


Fig. 2: The colour-colour diagram of the sample with VRI photometry from Magnier et al. (1992). The objects with measured magnitude in B are plotted on the  $(B-V)/(V-I)$  diagram as well. The symbols are the same as in Fig. 1.

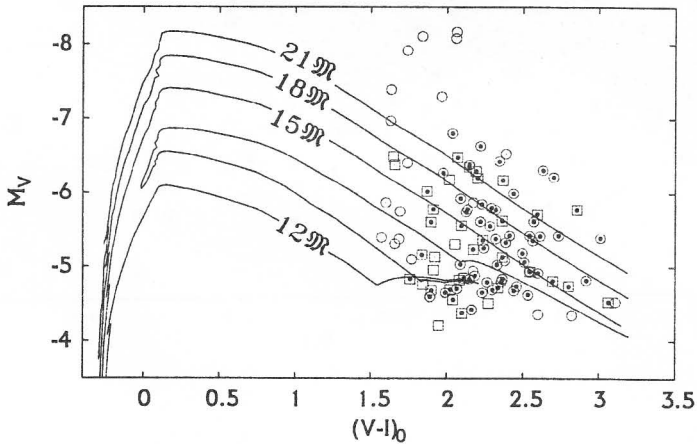


Fig. 3: The dereddened RSG-candidates from Magnier et al. (1992) (circles) and Massey (1998) (squares) on the colour-magnitude diagram. The evolutionary tracks for 12, 15, 18 and 21 solar masses and  $Z = 0.02$  (solid lines) are plotted. The filled symbols are the subsample selected for study of the metallicity gradient and the gas-to-dust ratio.

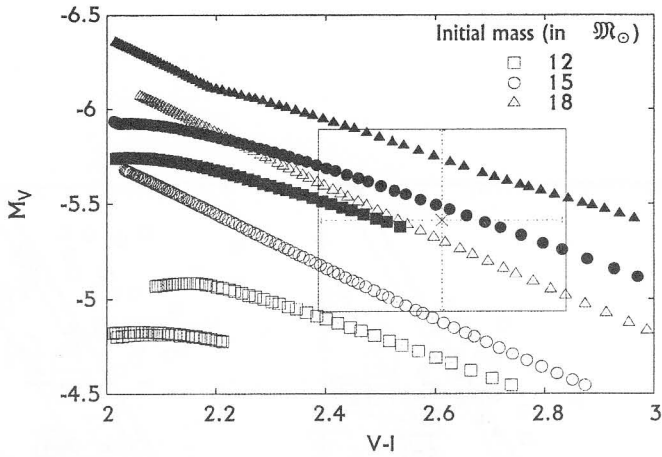


Fig. 4: The ‘bullets-method’ for estimation of star’s metallicity. A set of evolutionary tracks for metallicities  $Z = 0.012$  (filled symbols) and  $Z = 0.02$  (open symbols) and three different initial masses (squares, circles and triangles) are given. The error bars in colour and absolute magnitude determine the area for counting the points of equal timesteps for given  $Z$  (see text).

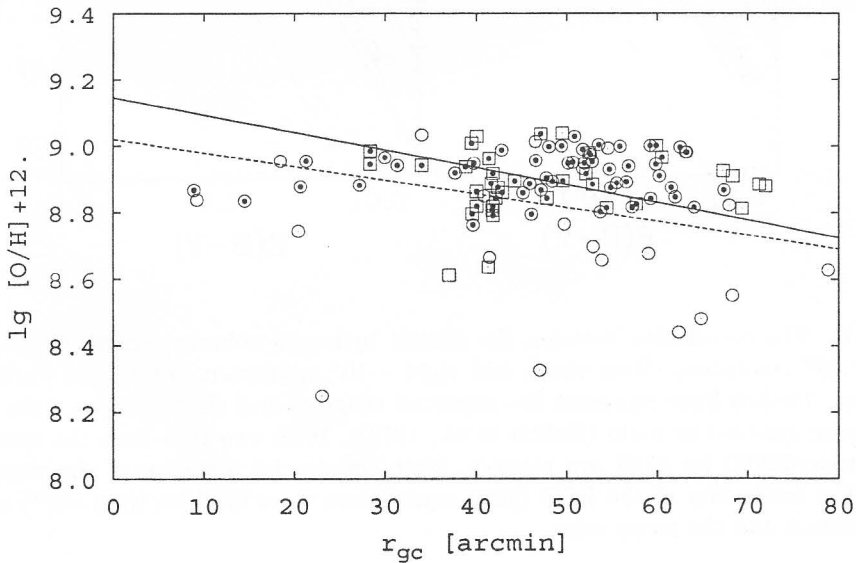


Fig. 5: Metallicity of individual stars in M31 (in units of oxygen abundance) versus their galactocentric distance. The symbols are the same as in Fig. 3. The mean abundance gradients derived by Galarza, Waltherbos & Braun (1999) (solid line) and Smartt et al. (2001) (dashed) are plotted for comparison.

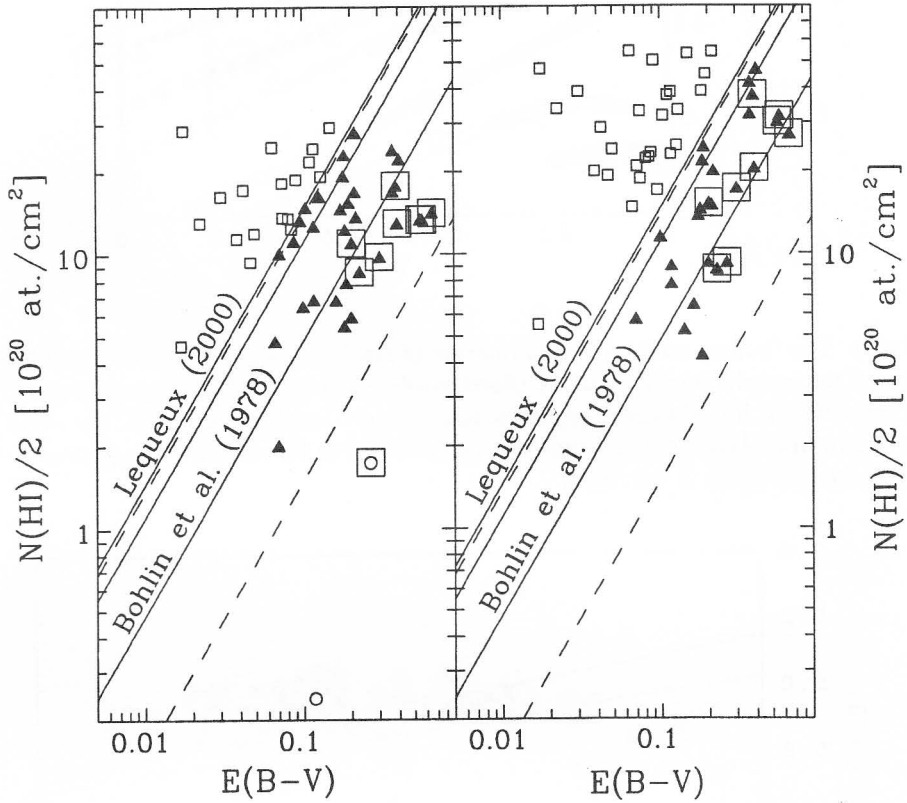


Fig. 6: The correlation between the atomic hydrogen column density  $N(\text{HI})$  (left -  $24 \times 36''$  resolution, Westerbork and right -  $10''$  resolution, VLA) and extinction  $E_{B-V}$ . Dashed lines represent the expected range of and the thick one - the mean Galactic gas-to-dust ratio (Bohlin et al., 1978). With two thin lines the results of Lequeux (2000) for M31 are plotted. Note the crucial influence of the resolution and the luminosity of the RSG (large squares are stars brighter than  $-6^m$ ) on the correlation and the mean value.



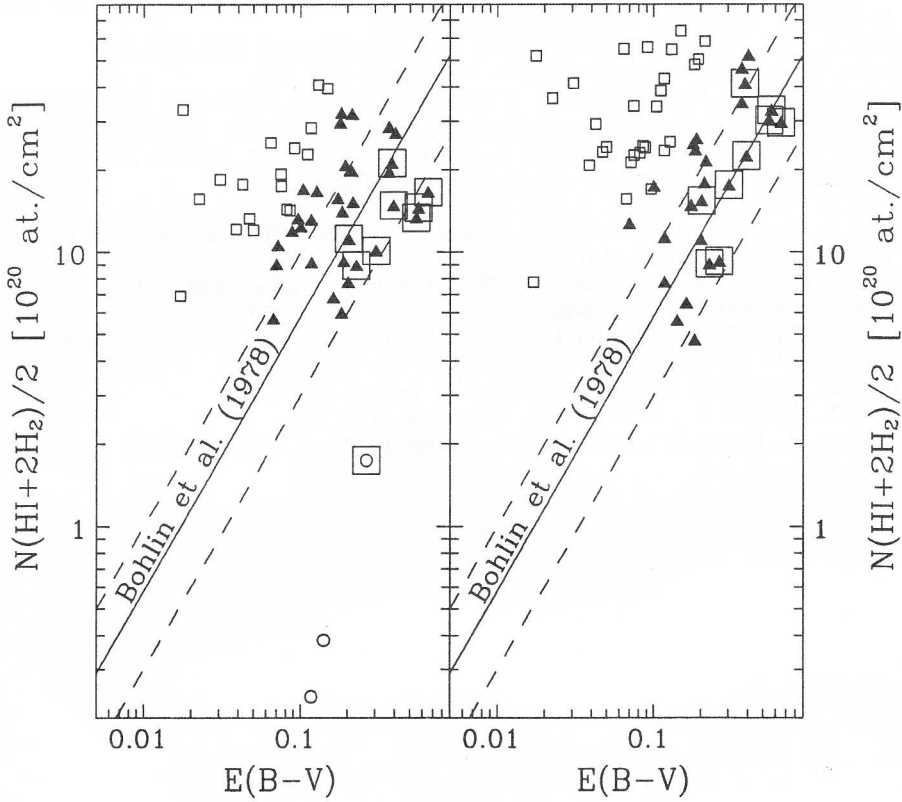


Fig. 7: The same as in Fig. 6, but for the half of the hydrogen total column density. The molecular fraction was added, assuming constant  $X(\text{CO})$  conversion factor (Strong & Mattox, 1996). Note the absence on both the right hand panels of open circles corresponding to stars, embedded in unresolved small clouds.

References

- Anders, E., Grevesse, N. : 1989, *Geochim. Cosmochim. Acta*, **53**, 197.
- Berkhuijsen, E., Humphreys, R. : 1989, *Astron. Astrophys.*, **214**, 68.
- Bohlin, R., Savage, B., Drake, J. : 1978, *Astrophys. J.*, **224**, 132.
- Brinks, E., Shane, W. : 1984, *Astron. Astrophys.*, **55**, 179.
- Galarza, V., Walterbos, R., Braun, R. : 1999, *Astron. J.*, **118**, 2775.
- Guelin, M., Nieten, C., Neininger, N., Muller, S., Lucas, R., Ungerechts, H., Wielebinski, R. : 2000, *Proc. 232. WE-Heraeus Seminar*, Bad Honnef, Germany; Eds. E. Berkhuijsen, R. Beck, R. Walterbos. Shaker, Aachen, 2000, 15.
- Hurley, J., Pols, O., Tout, C. : 2000, *Mon. Not. Royal Astron. Soc.*, **315**, 543.
- Lejeune, T., Schaerer, D. : 2001, *Astron. Astrophys.*, **366**, 538.
- Lequeux, J. : 2000, *Proceedings 232. WE-Heraeus Seminar*, 22-25 May 2000, Bad Honnef, Germany; Eds. E. Berkhuijsen, R. Beck, R. Walterbos. Shaker, Aachen, 2000, 63.
- Magnier, E., Lewin, W., van Paradijs, J., Hasinger, G., Jain, A., Pietsch, W., & Truemper, J. : 1992, *Astron. Astrophys. Suppl. Series*, **96**, 379.
- Massey, P. : 1998, *Astrophys. J.*, **501**, 153.
- Pagani, L., Lequeux, J., Cesarsky, D., Donas, J., Milliard, B., Loinard, L., Sauvage, M. : 1999, *Astron. Astrophys.*, **351**, 447.
- Salasnich, B., Bressan, A., Chiosi, C. : 1999, *Astron. Astrophys.*, **342**, 131.
- Schlegel, D., Finkbeiner, D., Davis, M. : 1998, *Astrophys. J.*, **500**, 525.
- Smartt, S., Crowther, P., Dufton, P., Lennon, D., Kudritzki, R., Herrero, A., McCarthy, J., Bresolin, F. : 2001, *Mon. Not. Royal Astron. Soc.*, **325**, 257.
- Stanek, K., Garnavich, P. : 1998, *Astrophys. J. Letters*, **503**, L131.
- Strong, A., Mattox, J. : 1996, *Astron. Astrophys.*, **308**, L21.
- Walterbos, R., Braun, R. : 1992, *Astron. Astrophys. Suppl. Series*, **92**, 625.